Low-temperature spin-state transition in $LaCoO_3$ investigated using resonant x-ray absorption at the Co *K* edge

M. Medarde,[1,2] C. Dallera,[3] M. Grioni,[4] J. Voigt,[2,5] A. Podlesnyak,[2] E. Pomjakushina,[1,2] K. Conder,[1,2] Th. Neisius,[6] O. Tjernberg,[7] and S. N. Barilo[8]

[1]*Laboratory for Developments and Methods, Paul Scherrer Institute, 5232 Villigen PSI, Switzerland*

[2]*Laboratory for Neutron Scattering, ETH Zurich and PSI, 5232 Villigen PSI, Switzerland*

[3]*INFM, Dipartimento di Fisica, Politecnico di Milano, piazza Leonardo da Vinci 32, 20133 Milano, Italy*

[4]*Institut de Physique des Nanostructures, Ecole Polytechnique Fédérale, 1015 Lausanne, Switzerland*

[5]*Institut für Festkörperphysik des Forschungszentrums Jülich, 52425 Jülich, Germany*

[6]*European Synchrotron Radiation Facility, Boîte Postale 220, 38043 Grenoble Cédex, France*

[7]*Laboratory of Materials and Semiconductor Physics, Royal Institute of Technology, Electrum 229, S-164 40 Kista, Sweden*

[8]*Institute of Solid State and Semiconductor Physics, National Academy of Science, Minsk 220072, Belarus*

(Received 2 June 2005; revised manuscript received 21 December 2005; published 15 February 2006)

$LaCoO_3$ displays two broad anomalies in the DC magnetic susceptibility χ^{DC}, occurring, respectively, around 50 K and 500 K. We have investigated the first of them within the 10 K$<T<$RT temperature range using Co $K\alpha_1$ x-ray absorption spectroscopy (XAS) in the partial fluorescence yield mode. In contrast with previous O *K*-edge XAS reports, our data show the existence of abrupt changes around 50 K which can be nicely correlated with the anomaly in χ^{DC}. To our knowledge, this is the first time that a clear, quantitative relationship between the temperature dependence of the magnetic susceptibility and that of the XAS spectra is reported. The intensity changes in the preedge region, which are consistent with a transition from a lower to a higher spin state, have been analyzed using a minimal model including the Co 3*d* and O 2*p* hybridization in the initial state. The temperature dependence of the Co magnetic moment obtained from the estimated e_g and t_{2g} occupations could be satisfactorily reproduced. Also, the decrease of the Co 3*d* and O 2*p* hybridization by increasing temperature obtained from this simple model compares favorably with the values estimated from thermal evolution of the crystallographic structure.

DOI: 10.1103/PhysRevB.73.054424 PACS number(s): 75.30.Wx, 61.10.Ht, 78.70.Dm, 75.30.Et

I. INTRODUCTION

Co oxides have been the subject of an increasing number of investigations since the report of magnetoresistivity ratios of 30% in the oxygen-defective perovskites[1] $R\mathrm{BaCo_2O_{5.4}}$ (R=Eu, Gd) and especially after the recent discovery of superconductivity in a Co-based layered compound ($\mathrm{Na_xCoO_{2y}H_2O}$, x=0.35, y=1.3, T_C=5 K).[2] Besides the challenging phenomena displayed by these novel Co compounds, the lattice, electronic and magnetic properties of the prototypical perovskite $LaCoO_3$ continue to attract the attention of scientists since the late 1950s.[3–6] The main controversy is still centered on the origin of the two broad transitions in the magnetic susceptibility occurring around T_1 =50 K and T_2=500 K. Although no traces of cooperative magnetic ordering have been found down to 1.5 K,[7,8] the effective Co^{3+} paramagnetic moment μ^{eff} displays a rather unusual, two-step-like temperature dependence.[9] It is practically zero below 35 K, it increases continuously until 100–110 K, then displays a broad plateau and increases further until T_2, where a second plateau is observed.

Both magnetic anomalies were first interpreted by Goodenough[3,10,11] as spin-state transitions. In the particular case of $LaCoO_3$, the possibility of having Co^{3+} in different spin states as a function of temperature has been attributed[3] to the close values of the intra-atomic exchange energy (J_H) and the crystal field splitting ($10Dq$) at the Co sites. Hence, depending on the relative values of J_H and $10Dq$, the low-spin (LS) ($t_{2g}^6e_g^0$, S=0) state can be more stable than the Hund's rule predicted high-spin (HS) ($t_{2g}^4e_g^2$, S=2) state.

Goodenough[11] attributed the 50 K anomaly to a thermally activated spin transition from a nonmagnetic LS state to a paramagnetic HS state. With increasing temperature, the HS population increase at the expense of the low-temperature LS up to a 1:1 ratio and, at this stage, the formation of a stable ordered LS-HS spin-state array would give rise to the first plateau. The second anomaly, which was associated with a semiconductor-to-metal transition, was interpreted as arising from the destruction of the spin-ordered state due to the increased mobility of the e_g electrons, accompanied by the transition to the HS state of the remaining 50% LS ions.

In spite of the anomalies observed in the thermal expansion,[4,12] in the cell parameters,[10] as well as in some interatomic distances[8] and phonon modes[13,14] at the magnetic transitions, most x-ray and neutron diffraction studies failed to detect the expected symmetry change associated with the formation of the spin-ordered state. To our knowledge, the only experimental evidence comes from a recent x-ray single crystal diffraction work,[5] as well as from the neutron pair density function (PDF) studies from Louca *et al.*[15] Moreover, the presence of the HS state below 400 K is difficult to reconcile with the results of x-ray absorption (XAS) and photoemission experiments. The main discrepancy is the weak temperature dependence of the preedge structure of O 1*s* XAS spectra across T_1,[16] which is related to the Co 3*d* unoccupied density of states and, therefore, to the variations in

the e_g and t_{2g} occupations associated to the different Co^{3+} spin states.

In Goodenough's picture, the decrease of the t_{2g} occupation should be equal to the increase of the e_g occupation at both T_1 and T_2. Unexpectedly, only very small changes could be detected around the first transition, while large intensity variations were clearly observable around 500 K.[16,17] Although this observation could be due to the fact that $T_1 = 50$ K was not actually reached in these studies [the authors assumed $T_1 = 100$ K, the lowest measured temperatures being 80 K (Ref. 16) and 55 K (Ref. 17)], this trend has been confirmed by more recent works reaching temperatures as low as 20 K.[18] The situation seems to be somehow better at the Co *K* edge, where, in spite of clear preedge differences between the spectroscopic response at T_1 (Ref. 18) and T_2 (Ref. 19), the reported changes at the low-temperature spin transition are larger than at the O *K* edge. Unfortunately, the resolution of these measurements is relatively poor. Also, only a limited data set is presented (20 and 300 K), making it difficult to correlate the observed changes with the anomaly in the magnetic susceptibility.

To explain these observations, it was first suggested that the anomaly at T_1 is not a spin transition and that the LS $\rightarrow$HS crossover actually occurs at T_2.[16] An alternative model proposed the existence of an intermediate-spin (IS) ($t_{2g}^5 e_g^1$, $S=1$) state and interpreted the two anomalies as thermally activated LS$\rightarrow$IS and IS$\rightarrow$HS transitions.[17] The justification of the higher stability of the IS state as compared to that of the HS, which contradicts the predictions of classical ligand field theory,[20] was mainly based on the calculations of Korotin *et al.*[20] In the case of XAS, this approach had the advantage of predicting smaller spectroscopic changes at 100 K but, since the effects at 500 K were also expected to decrease, the unequal spectroscopic responses at T_1 and T_2 remained unexplained.

Interestingly, since its report in 1997,[17] the LS$\rightarrow$IS$-$IS $\rightarrow$HS model has been successfully applied to the interpretation of a number of different experiments[4,5,8,13,14] and has become the most widely accepted framework for the transitions. On the other hand, recent theoretical works, among them those of Radwanski and Ropka,[21–23] have returned to the HS scenario. These authors pointed out that the trigonal crystal field and the spin-orbit coupling may be important in forming the first magnetic excited state, which would arise from the splitting of the HS state. Recent electron spin resonace[24] (ESR) and inelastic neutron scattering measurements[25] seem to be consistent with this hypothesis.

Since the debate around x-ray spectroscopies has not yet been satisfactorily settled neither for this compound nor in other perovskite-related Co oxides,[26] the purpose of the present work is to reinvestigate the low-temperature transition of $LaCoO_3$ using a different, more suitable x-ray spectroscopic technique. The motivation for new resonant absorption measurements at the Co *K* edge is threefold. Firstly, x-ray absorption in the partial fluorescence yield (PFY-XAS) mode leads to a substantial improvement in resolution with respect to total fluorescence yield (TFY), allowing the observation of fine details in the electronic structure. Secondly, the *K* edges of 3*d* transition metals display a remarkable sensitivity to the valence electron distribution of the absorbing atom, illustrated, e.g., by recent experimental and theoretical work on manganese oxides.[27–29] Lastly, hard x-rays provide more reliable information about bulk properties compared with surface-sensitive O 1*s* XAS. Since a low-temperature contribution, usually attributed to localized magnetic moments from the surface (probably HS Co^{2+} in either pyramidal or tetrahedral coordination) is systematically observed in the magnetic susceptibility data of both single crystal and powder samples,[4,6,11,17,30] the choice of a high-energy technique and the use of single crystals (which display a smaller surface-to-bulk ratio) was in this case crucial.

In this work, we report temperature-dependent measurements, performed on a high quality $LaCoO_3$ single crystal, which clearly prove the sensitivity of Co $K\alpha$ PFY-XAS to the magnetic anomaly at T_1. In contrast with previous O *K* and Co *K*-edge studies, our data display dramatic changes as a function of temperature at several points of the edge, which can be nicely correlated with those of the effective Co paramagnetic moment derived from susceptibility measurements. We take advantage of the improved visibility of the preedge structures in the PFY compared to conventional XAS spectra to obtain new information on the local configuration of the Co ions. We interpret the experimental data within a minimal model which includes the Co 3*d* and O 2*p* hybridization in the initial state. The temperature dependence of both the Co 3*d* - O 2*p* hybridization and the Co magnetic moment can be satisfactorily described within this formalism. However, due to the roughness of our approximations, the absolute values of the e_g and t_{2g} occupations obtained from this analysis should be considered with caution. Although this fact makes difficult a definitive statement about the nature of the involved spin states, our results are consistent with a thermally driven hole transfer from the e_g into the t_{2g} orbitals.

II. EXPERIMENT

The $LaCoO_3$ single crystal used in this work was grown by the floating-zone method. Thorough mixtures of La_2O_3 and Co_3O_4 (99.99% purity) were heated in air at 1000–1200 °C during more than 70 h with several intermediate grindings. The resulting $LaCoO_3$ powder was hydrostatically pressed into rods (8 mm in diameter and ~60 mm in length) and sintered at 1300 °C during 30 h. The crystal growth was carried out under moderate oxygen pressure (6 bar) using an optical floating zone furnace with four 1000 W halogen lamps. The feeding and seeding rod were rotated at about 20 rpm in opposite directions to ensure the liquid homogeneity between them, the growing rate being 5 mm/h.

Two adjacent wafers of 6.3 mm diameter and 1 mm thick were cut from the as-grown boule. The first one was pulverized and used for x-ray characterization and O content determination. A room temperature x-ray diffraction pattern was collected on a Siemens D500 θ-2θ powder diffractometer using Cu-$K\alpha$ radiation. Rietveld refinements were consistent with a rhombohedral unit cell of $R-3c$ symmetry [$a = 5.4433(1)$Å, $c = 13.0932(4)$Å], in agreement with most previous reports.[8,10] No evidence of impurities was found in the limit of x-ray detection. The oxygen content, as determined

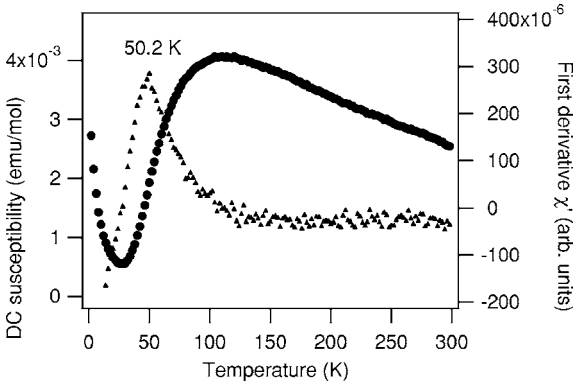

FIG. 1. Full dots: Temperature dependence of the molar magnetic DC susceptibility of the $LaCoO_3$ single crystal measured at $H=10$ kOe. Full triangles: First derivative showing the maximum at $T=50.2$ K.

from thermogravimetric hydrogen reduction, was 3.00 ± 0.01.

The second wafer was used for the x-ray spectroscopic experiments. It was glued on a copper plaquette with silver epoxy and mounted on a closed-cycle He cryostat (stability about 2 K). The measurements were performed on beamline ID26 at the European Synchrotron Radiation Facility in Grenoble, (ESRF), France using radiation from two undulator sources monochromatized by a Si(220) double crystal. X-ray absorption spectra in the TFY mode were collected at the Co K absorption edge ($h\nu_{in}=7.709$ keV) using a Si diode detector. For PFY measurements, the beam scattered by the sample was analyzed by a Rowland circle spectrometer equipped with a spherically bent Si(531) crystal and detected by a photoavalanche diode. The scattering angle was 90 degrees to minimize Thomson scattering, and the overall energy resolution was better than 1.5 eV. The intensity of the Co $K\alpha_1$ fluorescence ($2p\rightarrow1s$, $h\nu_{out}=6.930$ keV) was measured at several temperatures between RT and 10 K (cooling rate of approximately 4.5 K/min) while scanning the energy of the incident beam between 7.705 and 7.730 keV.

A small piece of the second wafer (0.03548 g) was cut after the ESRF experiments and used for DC susceptibility measurements. They were performed on a commercial Quantum Design Physical Properties Measuring System (PPMS) device in the $2\text{ K}<T<\text{RT}$ temperature range under a magnetic field of 10 kOe.

III. RESULTS

A. DC magnetic susceptibility

The magnetic susceptibility of our $LaCoO_3$ crystal is displayed in Fig. 1. It shows a broad maximum around $T_M=112$ K, and a minimum at $T_m=26$ K, in agreement with previous studies.[4,6,11,17,30] The only significant difference appears in the low-temperature region ($T<35$ K), which is affected by magnetic impurities and/or Co atoms at the sample surface.[6,11] The $\chi(T_m)/\chi(T_M)$ ratio, which gives an indication of the impurities and/or the surface contribution compared to that of bulk Co in $LaCoO_3$ is ≈0.125, much smaller than the values previously reported for both powder [0.28 (Ref. 11), 0.43 (Ref. 17)] and single crystal [0.33 (Ref. 4), 0.29 (Ref. 6), 0.17 (Ref. 30)] samples. The first derivative (see Fig. 1) exhibits a sharp cusp at $T_1=50.2$ K, which in the following sections will be used to designate the transition temperature. According to recent[24] ESR and inelastic neutron scattering measurements,[25] the gap energy E_g between the ground state and the first excited state is about 10–12 meV (119–140 K). T_1, which coincides with the anomalies observed in the thermal expansion[4] and in the phonon frequencies,[13,14] thus corresponds to $E_g/2$.

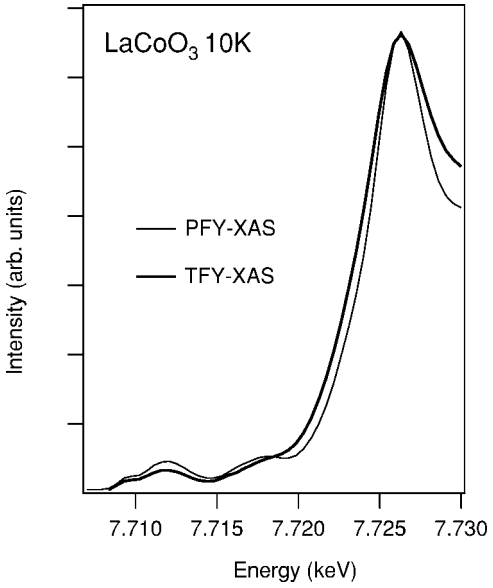

FIG. 2. Comparison of the TFY and PFY Co $K\alpha$ XAS spectra at 10 K.

B. X-ray absorption

The Co K-edge spectra of $LaCoO_3$ at 10 K measured in the total and partial fluorescence yield modes are shown in Fig. 2. They basically agree with those published by Thornton *et al.*,[19] Haas *et al.*,[31] and Toulemonde *et al.*[18] but the improvement in resolution of our PFY data is evident for the whole energy range. For example, the structures between 7.715 and 7.720 keV (labeled as $G3$ and $G4$, see Fig. 3), which are hardly distinguishable in the TFY mode, are particularly well resolved using PFY detection.

The measured PFY-XAS Co $K\alpha_1$ spectra of $LaCoO_3$ at 10 K and RT, divided by the incoming photon intensity and normalized at $E=7.7282$ keV, consistent with Ref. 18, are shown in Fig. 3(a). The difference patterns obtained by subtraction of the temperature-dependent data from the RT spectrum are displayed in Fig. 3(b). To be noted is the existence of several crossing points, confirming the correctness of the normalization procedure. Also, the existence of changes in the absorption cross section by increasing temperature is clearly observed. The most important of them consists of a large displacement of the absorption maximum $G6$ toward lower energies, which is accompanied by modest energy shifts of the same sign in the $G2$, $G3$, $G4$, and $G5$ features. The small preedge structure $G1$ is found in contrast to shift

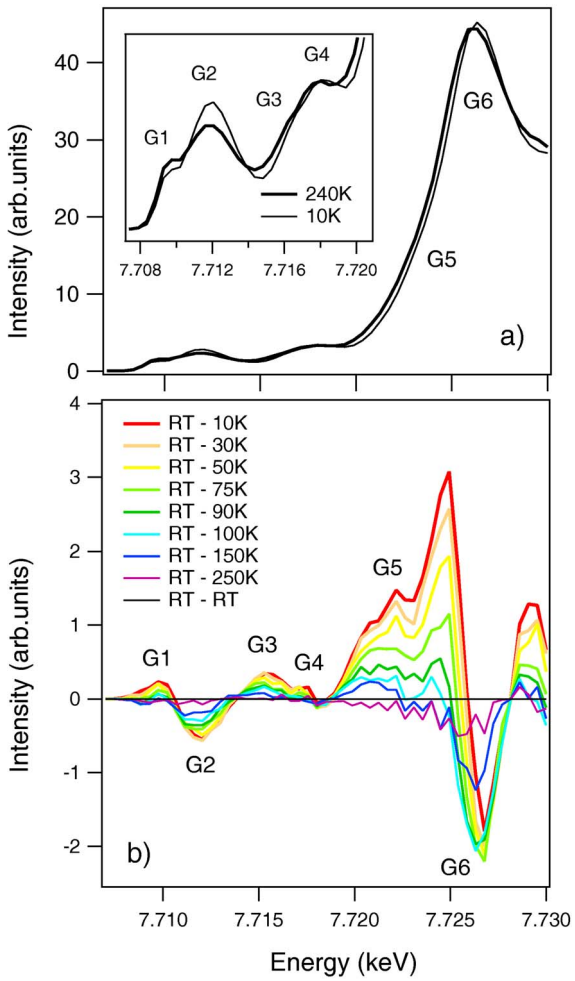

FIG. 3. (Color online) (a) Co $K\alpha$ PFY-XAS spectrum of $LaCoO_3$ at 10 K and RT. Inset: Detail of the preedge structure. (b) Difference patterns obtained by subtracting the PDF-XAS spectra at different temperatures from the RT data.

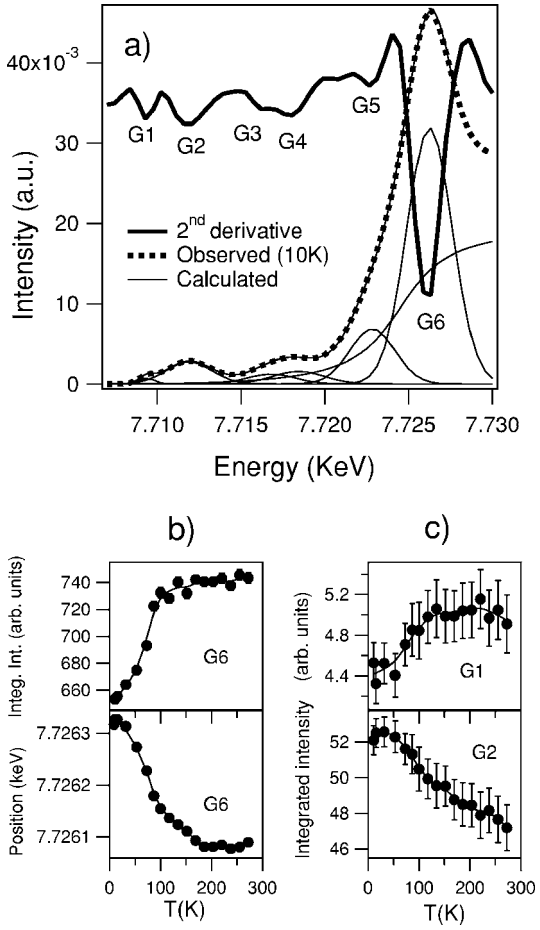

FIG. 4. (a) Dottted line: Co $K\alpha$ PFY-XAS spectrum of $LaCoO_3$ at 10 K. Solid line: Best fit as described in the text. The individual Gaussian and arctangent contributions are also displayed, as well as the second derivative of the 10 K spectrum (bold solid line). (b) Temperature dependence of the integrated intensity and the energy position of the *G*6 feature. (c) Temperature dependence of the integrated intensities of the *G*1 and *G*2 features. Solid lines in (b) and (c) are guides for the eye.

in the sense of higher energies (see Sec. IV B). An increase of the absorption cross section is also observed in all features with the exception of *G*2, which decreases by increasing temperature.

In order to evaluate the precise energy positions and integrated intensities of the six features, we fitted the whole spectra (between 7.705 and 7.727 keV) with an arctangent plus six Gaussians. The shape of the arctangent was determined from a RT PFY-XAS spectrum collected over a wider energy range (between 7.700 and 7.765 keV) and fixed for the subsequent refinements, whereas the Gaussian positions were located at the minima of the of the spectra's second derivative [see Fig. 4(a)].

The calculated values of the integrated intensity and the energy position of the *G*6 feature as a function of temperature are displayed in Fig. 4(b). According with the conclusions derived from the difference spectra, an increase of the integrated intensity and a displacement of the energy position toward lower energies are clearly observed by heating. The integrated intensities of the *G*1 and *G*2 features are displayed in Fig. 4(c). As in the case of *G*6, their temperature dependence coincides well with that inferred from the difference patterns. Moreover, a clear anomaly is observed in all cases at a temperature close to T_1, suggesting a close relationship between observed changes in the PFY-XAS spectra and the magnetic transition. As far as we know, this is the first time that a clear, quantitative correlation between the temperature dependence of the magnetic susceptibility and that of the XAS spectra is reported.

IV. DISCUSSION

A. Origin of the different features

According to the electric dipole selection rules, the main contribution to the Co *K* edge ($E > 7.715$ keV) involves the excitation of Co 1*s* core electrons into empty Co states of 4*p* symmetry. The origin of the small double-peak structure between 7.705 and 7.715 keV (*G*1 and *G*2 in Fig. 3), which is also observed in the preedge region of XAS spectra of other first row transition metal compounds, is more complex. Shulman *et al.*[32] were the first to assign it to a $1s \rightarrow 3d$ transition

after observing that Zn(II), a d^{10} system, did not display this feature. However, for materials with a transition metal in a centrosymmetric environment, a $1s \rightarrow 3d$ transition is dipole forbidden by parity considerations and this structure should be absent. Interestingly, a very weak preedge feature is still experimentally observed in such compounds. Hence, and due to the fact that, for energies above a few keV, nondipole terms begin to contribute to absorption cross sections, electric quadrupole transitions were suggested as the most likely mechanism in such cases. Experimentally, the electric quadrupole nature of the preedge feature has been probed in a few cases by analyzing the angular dependence of the $1s \rightarrow 3d$ transition intensity, although, due to the complexity of the procedure, as well as the need of single crystals, the number of such studies (as, for example, the remarkable measurements conducted by Hahn *et al.*[33]) is scarce.

For compounds containing 3*d* transition metals in noncentrosymmetric environments, it has been found that the preedge features are far more intense than in their centrosymmetric counterparts (2 to 5 times, see Ref. 34 and references therein). This increase in intensity has been attributed to metal 4*p* mixing into the 3*d* orbitals, which, by providing some electric dipole-allowed $1s \rightarrow 4p$ character, contributes with extra intensity which is added to that of the quadrupolar channel. Since electric dipole transitions are typically up to 100 times stronger than those enabled by the electric quadrupole mechanism, 4*p* mixing into the 3*d* orbitals (typically below 10%) may have a significant effect on the intensity of the $1s \rightarrow 3d$ feature. A good example was reported by Dräger *et al.*,[35] who, using angle-resolved polarized x-ray absorption on the Fe *K* edge of haematite single crystals, showed that the intensity of the preedge feature was mostly dipolar in origin.

In the case of $LaCoO_3$, and due to the uncertainty about the existence or not of an inversion center at the Co sites, the nature (dipolar and/or quadrupolar) of the preedge feature cannot be unambiguously established. If, as suggested by all diffraction studies, the low-temperature ($T < T_1$) space group is $R-3c$, the point group of the CoO_6 octahedra is S_6 (centrosymmetric), and the intensity of the *G*1-*G*2 feature will be purely quadrupolar in origin. If the symmetry center at the Co positions is lost above T_1 due to structural changes induced either by LS-HS ordering[11] or IS Jahn-Teller distortions[15] (the Co^{3+} IS configuration is Jahn-Teller active), an increase of the overall preedge intensity would be expected. However, as it will be shown in Sec. IV B, the *G*1 + *G*2 integrated intensity decreases monotonically with temperature. The deviation from centrosymmetry above T_1, if existing, is expected to be very small. This agrees with the conclusions of Raccah and Goodenough[10] and Maris *et al.*,[5] which proposed centrosymmetric space groups to describe the high-temperature phase of $LaCoO_3$ ($R-3$ and $I2/a$, respectively). We thus conclude that the degree of *p*-*d* mixing in the preedge region is most likely modest above T_1, favoring a primarily quadrupolar origin for the *G*1-*G*2 feature.

We come now to the main edge region (7715–7730 eV), which, as it was already mentioned, corresponds to the excitation of Co 1*s* core electrons into empty Co states of 4*p* symmetry. Although these states are not expected to be very sensitive to the anomaly at T_1, Fig. 3(b) clearly shows that the largest changes of the absorption cross section take place within this energy range. Moreover, both the integrated intensities and the positions of the *G*3 to *G*6 features display clear anomalies around 50 K [Fig. 4(b)], suggesting that the Co 4*p* states are also affected by the changes in the Co 3*d* occupation at the spin-state transition.

Briois *et al.*,[36] who studied the spin-state transition of an octahedral Fe II complex, observed also a strong temperature dependence of the main Fe *K*-edge features, which they could correlate with the structural modifications of the Fe environment at the transition. The breaking of the rhombohedral symmetry above T_1 described by Maris[5] and Louca[15] could also be at the origin of the anomalies of the energy positions and integrated intensities of the different features at the transition. A proper correlation between Co-O nearest-neighbor distances and energy positions is unfortunately not possible in our case. For this purpose, angle-resolved XAS measurements along the Co-O bonds are needed, but they will probably be very difficult to interpret due to the fact that $LaCoO_3$ single crystals are naturally twinned.

As in the case of the preedge structures, an alternative scenario assuming the existence of some kind of *p*-*d* mixing could be also applicable to the energy region between 7715 and 7730 eV. This mechanism, which yields a 3*d* contribution to the main edge through purely dipolar transitions, has been recently proposed to explain the large and unexpected changes observed in the Mn *K* edges of manganese perovskites displaying either charge and/or orbital ordering phenomena. The *p*-*d* mixing concerns the 3*d* and the 4*p* states of the central transition metal and the O 2*p* states if the final state wave functions are localized at the coordination polyhedron of the absorbing atom.[37] On the contrary, if the final state wave functions of the absorber can be considered to be so extended that they overlap with those of the neighboring transition metal (TM) atom, the *p*-*d* mixing (which can be achieved either directly or via the O 2*p* states) concerns in this case the 4*p* states of the absorber and the 3*d* states of the next neighbor TM atom.[29]

Although a rigorous theoretical calculation for the full (edge and preedge) spectra is beyond the scope of this work, the simple model presented in the forthcoming sections gives already some important hints for the interpretation of the spectra. In this analysis, we confine ourselves to the preedge region between 7.705 and 7.715 keV, where the relative contribution of the 3*d* states is expected to be larger.[29] Following the preceding discussion, it will be then assumed that the actual transition channel active in this energy range is mainly quadrupolar, the intensity of the preedge feature basically reflecting the features of the density of empty Co 3*d* states.

In Sec. IV B, the discrepancies between a purely ionic description of the local Co electronic structure and the experimental observations are presented. Co 3*d* - O 2*p* hybridization, which is included in Sec. IV C, leads to a significant improvement, although it fails to reproduce the absolute occupation numbers of the 3*d* orbitals. The results of the analysis are summarized in Sec. V, together with the failures of our simple model and some suggestions for further improvement.

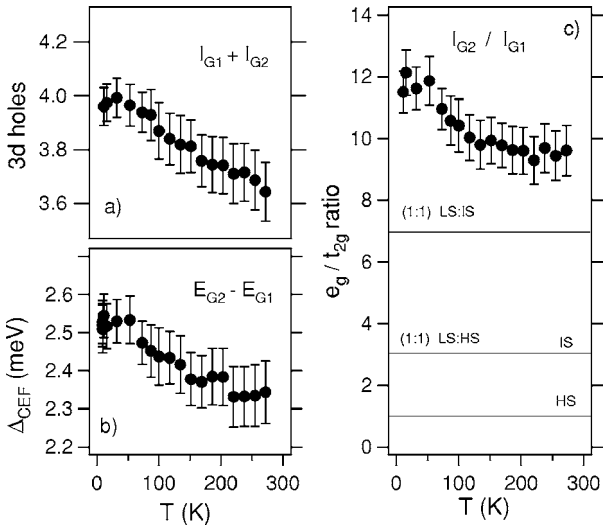

FIG. 5. Temperature dependence of (a) the sum of the integrated intensities of the $G1$ and $G2$ features. (b) The $G1$-$G2$ splitting. (c) The $G2/G1$ ratio.

B. Failures of the ionic description

As mentioned earlier, the preedge feature on the Co K edge of $LaCoO_3$, as well as that of the K edges of most $3d$ transition metal compounds in octahedral coordination consists of two (usually dissimilar) peaks. This double-peak structure, which is also observed in the preedge region of the O $1s$ XAS spectra for this kind of compounds,[38] has been related to the e_g ($G2$) and t_{2g} ($G1$) symmetry subbands arising from the octahedral (or quasioctahedral[39]) crystal splitting of the Co $3d$ orbitals.[38]

In a purely ionic description, the integrated intensity of the preedge feature intensity can be correlated with the number of empty Co $3d$ states. For Co^{3+}, the hole number is 4 for all spin states, so that the full $I_{G1}+I_{G2}$ preedge intensity should be independent of temperature. On the contrary, as shown in Fig. 5(a), a decrease of $I_{G1}+I_{G2}$ is observed by heating, with a net reduction of about 10% between 10 K and RT. This effect is due to the different temperature dependences of the integrated intensities of the two features [Fig. 5(a)] and cannot be explained in the framework of a purely ionic model.

The two preedge features can be directly assigned to t_{2g} and e_g crystal field states only in a single-particle picture, which neglects intra-atomic multiplet effects in the Co ion, the spin-orbit interaction, as well as the influence of the core hole potential. Nevertheless, following common practice, we will assume that the unresolved $G1$ and $G2$ manifolds mainly reflect transitions to t_{2g} and e_g orbitals, respectively. Their temperature-dependent energy separation, which defines an effective crystal field parameter $\Delta_{CEF}=E_{G2}-E_{G1}$ is displayed in Fig. 5(b). At RT, the value of Δ_{CEF} is $\approx$2.3 eV, in good agreement with the Co K-edge data of Toulemonde *et al.*[18] and Thornton *et al.*,[19] but it is about two times larger than the corresponding splitting observed in the O K edge ($\Delta_{CEF} \approx 1$ eV, in Refs. 16 and 18). This discrepancy, which has been observed in the case of other transition metal oxides (see Ref. 40 and references therein), has been attributed to smaller core-hole effects in the O K XAS, where the core hole is located on oxygen, whereas the states in the unoccupied bands just above the Fermi level have most weight on the metal sites.

Although the Δ_{CEF} values obtained from XAS at the O K edge are, in principle, expected to be closer to ground-state values, the larger sensitivity of this spectroscopy to surface Co may also lead to wrong results. Yan *et al.*[30] attributed the low-temperature tail in the magnetic susceptibility to the presence of magnetic surface Co in either pyramidal or tetrahedral coordination. Since for this environment, the Δ_{CEF} value is expected to be substantially smaller than in the case of octahedral Co, the amount of surface Co contributing to the absorption cross section could also be at the origin of the reported differences between the Co and O K edges.

Several estimates of Δ_{CEF} can be found in the literature, but its temperature dependence has not been reported so far. Figure 5(b) shows the Co K-edge values of Δ_{CEF} between 10 K and RT. As expected from thermal expansion, the effective crystal field splitting decreases by increasing temperature, the difference between 10 K and RT being about 200 meV. While this trend supports the possibility of a thermally driven spin transition at T_1, a definitive statement can only be made after comparing the experimental I_{G2}/I_{G1} ratios with those expected for the different spin states.

In Fig. 5(c), we have represented the values of the e_g/t_{2g} hole ratio for the IS (3:1), HS (2:2), 50%LS+50%HS (3:1) and 50%LS+50%IS (7:1) states together with the experimentally obtained I_{G2}/I_{G1} ratio as a function of temperature. Clearly, our data show serious discrepancies with Goodenough's model, especially at low temperature. If, as proposed by this author, the ground state of Co is LS (4:0), the t_{2g} feature is expected to be absent below 35 K, giving rise to an infinite I_{G2}/I_{G1} ratio. Since the value of I_{G2}/I_{G1} at 10 K is close to 12 due to the existence of a nonzero $G1$ intensity at this temperature, we conclude that a certain amount of another higher spin state (either IS or HS) is already present at 10 K. At higher temperatures, where a 50% mixture of either LS:HS or LS:IS is expected to occur, we observe a I_{G2}/I_{G1} ratio close to 9, which, in spite of the relatively large discrepancy, would, in principle, favor the LS$\rightarrow$IS scenario.

The observation of a non-zero-spin Co at 10 K, which contradicts Goodenough's picture, as well as the results of the magnetic susceptibility[4] and neutron paramagnetic scattering measurements,[41] is very surprising and deserves further comment. Comparison of our $LaCoO_3$ spectra with other XAS data on LS Co^{3+} compounds could be quite instructive but, in view of the lack of high-resolution experimental data, we chose instead a series of isoelectronic LS Fe^{2+} octahedral (centrosymmetric) complexes (Ref. 34). Due to their common $t_{2g}^6 e_g^0$ configuration, a single peak corresponding to quadrupolar $1s\rightarrow 3d$ transitions into the empty e_g states was expected in both cases, but it is only observed in the Fe^{2+} compounds.[34]

Since the values of the intra-atomic exchange J_H are probably very close for LS Fe^{2+} and LS Co^{3+}, the main difference between these materials and $LaCoO_3$ is the strength of the ground state (without core hole) crystal field splitting $10Dq$, which ranges from 2.5 to 3.5 eV for the Fe complexes[34] compared to (presumably) $\sim$1 eV for $LaCoO_3$. This last es-

timation is based on the Δ_{CEF} value measured at the O K edge,[16,18] which, as mentioned in previous paragraphs, is expected to be closer to the ground state value $10Dq$ than $\Delta_{CEF} \sim 2.3$ eV obtained from the Co K edge. If the anomaly at 50 K is due to a transition from LS to either IS or HS, the difference $10Dq - J_H$, which is a measure of the stability of the LS state with respect to higher spin states, is expected to be very small in the case of the cobaltite (an energy gap of 10–12 meV between the ground state and the first excited state has been reported[25,24]). Hence, $J_H \sim 10Dq \sim 1$ eV. Assuming that a similar J_H value also holds for the Fe complexes, we obtain $10Dq - J_H$ values between 1.5 and 3 eV. The LS configuration is therefore expected to be far more stable in these compounds than in $LaCoO_3$.

The observation of different features on the K preedges of the Co and Fe systems is presumably related to the different stabilities of the LS state in these materials. In the Fe complexes, the two spin configurations are well separated and, in consequence, very weakly hybridized. On the contrary, the very small energy gap between the ground state and the first excited state in $LaCoO_3$ yields to a mixing of spin states. The observation of the $G1$ feature in our 10 K spectra suggest that the configuration mixing could be enhanced in the XAS final state due to the presence of the core hole. A quantitative estimation of this effect, which will require a proper treatment of multiplet effects, the spin-orbit interaction, the crystal field, and the interaction of the $3d$ and $2p$ Co electrons with the core hole is unfortunately far from trivial.

C. Introducing covalency

The main discrepancies between the experimental data and the ionic description, namely, the different temperature dependence of the $G1$ and $G2$ features and the excessively large values of I_{G2}/I_{G1} above T_1 may be understood (at least qualitatively) taking into account the hybridization between the Co $3d$ states and the $2p$ orbitals of the oxygen ligands. Covalency is described by adding to the original ionic configuration an admixture of configurations in which one or more electrons have been transferred from the ligand to an e_g or a t_{2g} orbital. The three possible covalent spin states of Co in $LaCoO_3$ can then be written as

$$\Psi_i^{LS} = C(|t_{2g}^6\rangle + n_{e0}^{1/2} T_\sigma |t_{2g}^6 e_g^1 \underline{L}\rangle), \tag{1}$$

$$\Psi_i^{IS} = C(|t_{2g}^5 e_g^1\rangle + n_{e0}^{1/2} T_\sigma |t_{2g}^5 e_g^2 \underline{L}\rangle + n_{t0}^{1/2} T_\pi |t_{2g}^6 e_g^1 \underline{L}\rangle), \tag{2}$$

$$\Psi_i^{HS} = C(|t_{2g}^4 e_g^2\rangle + n_{e0}^{1/2} T_\sigma |t_{2g}^4 e_g^3 \underline{L}\rangle + n_{t0}^{1/2} T_\pi |t_{2g}^5 e_g^2 \underline{L}\rangle). \tag{3}$$

Here, C is a normalization constant and $\underline{L}$ represents a ligand hole. The numerical coefficients contain the corresponding number of holes n_{e0} and n_{t0}, as well as the matrix elements T_σ (σ bonds) and $T_\pi \sim (T_\sigma/2)$ (π bonds) for e_g and t_{2g} states, respectively. n_{e0} and n_{t0} take the values 4:0 (LS), 3:1 (IS), and 2:2 (HS). Note also that, for the sake of simplicity, the $\underline{L}^2$ configurations involving the transfer of two electrons from the O $2p$ to the Co $3d$ orbitals have been neglected. If, as discussed in previous sections, the intensity of the preedge structure is ascribed to a (primarily) quadrupolar $1s \rightarrow 3d$ transition, 11 different XAS final states (2 LS, 4 IS, and 5 HS) are possible. The relative intensities of the $G1$ and $G2$ features as a function of temperature can be evaluated by calculating the transition probabilities from the 3 ground states to these 11 final states. This task, which needs the explicit consideration of the full $3d$ multiplet for each spin state, the core-hole interaction as well as the proper point symmetry of Co in order to define the relevant crystal field splitting, is however far from trivial due to the large number of final states.

In the absence of such a full configuration interaction calculation, we can qualitatively estimate the effects of covalency considering the related but simpler case of the O K absorption, where a similar two-peak ($G1'$ and $G2'$) preedge structure reflects the density of empty $3d$ states of the TM ion.[38] Since in O $1s$ absorption, an electron is excited from the oxygen $1s$ core state to states with some oxygen $2p$ character, only configurations with a ligand hole $\underline{L}$ ($2p^5$) in the initial state can contribute to the spectrum, and the final states are:

$$\Psi_{f1} = |t_{2g}^{6-N} e_g^{N+1}\rangle, \tag{4}$$

$$\Psi_{f2} = |t_{2g}^{6-N+1} e_g^{N}\rangle, \tag{5}$$

with $N=0,1,2$ for LS, IS, and HS (note that in the case of LS, only Ψ_{f1} is accessible). Assuming the same O $2p$ and Co $3d$ hybridization in the initial and final state, one obtains for each spin configuration[38]

$$I_{G1'} \propto n_{t0} T_\pi^2 / Z, \tag{6}$$

$$I_{G2'} \propto n_{e0} T_\sigma^2 / Z, \tag{7}$$

with $Z=(1+n_{t0}T_\pi^2+n_{e0}T_\sigma^2)$. The $G1'/G2'$ intensity ratio is now $I_{G2'}/I_{G1'}=4n_{e0}/n_{t0}$, that is, four times larger than in the ionic case ($I_{G2'}/I_{G1'}=n_{e0}/n_{t0}$). Covalency enhances the intensity of the transitions to the e_g manifold by a factor of 4 relative to the t_{2g} counterpart, reflecting the factor of 2 between their respective transfer integrals. A similar enhancement operates for the K-edge spectra, and it is remarkable that the deviations from the $G1/G2$ ionic picture observed at the Co K-edge can be largely accounted for by these simple considerations.

We want now to calculate the actual (covalent) number of holes into the e_g and t_{2g} orbitals, that we will denote as n_e and n_t. The main difference between them and the ionic hole numbers n_{e0} and n_{t0} is that $n_{e0}+n_{t0}=4$, whereas $n_e+n_t=n=4-p$ (p is the number of O $2p$ holes) due to the transfer of p electrons from the O $2p$ into the Co $3d$ orbitals. Doing some further algebra, it is easy to show that

$$n_e = [n_{e0} + n_{e0}T_\sigma^2(n_{e0}-1) + n_{t0}n_{e0}T_\pi^2]/Z, \tag{8}$$

$$n_t = [n_{t0} + n_{t0}n_{e0}T_\sigma^2 + n_{t0}T_\pi^2(n_{t0}-1)]/Z, \tag{9}$$

and using the relationship $I_{G1'}+I_{G1'} \propto 1-(1/Z)$, we obtain

$$n_{t0} - n_t \propto I_{G1'}, \tag{10}$$

$$n_{e0} - n_e \propto I_{G2'}, \tag{11}$$

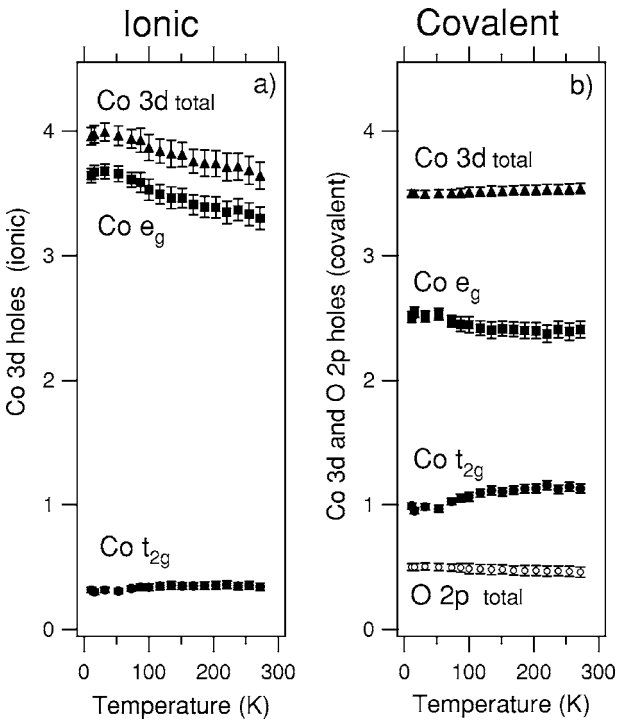

FIG. 6. Number of t_{2g} and e_g holes as a function of temperature in the ionic (a) and covalent (b) models.

$$4-(n_e+n_t)=4-n\propto(I_{G2'}+I_{G1'}). \tag{12}$$

Assuming $G2/G1=G2'/G1'$, Eqs. (10) to (12) describe the temperature dependence of the covalent holes n_e, n_t, and n. In order to get numerical values, the integrated intensities I_{G1} and I_{G1} should be, respectively, normalized to the covalent hole numbers of the e_g and t_{2g} orbitals at 10 K. The results obtained for a particular case [$4-n(10\ \mathrm{K})=0.5$, that is, 0.5 electrons transferred from the O $2p$ to the Co $3d$ orbitals at 10 K] are displayed in Fig. 6(b) together with the results of the ionic model [Fig. 6(a)]. The increasing (decreasing) rates of n_e and n_t are now approximately the same, and a small *increase* of the total number of Co $3d$ holes n as a function of temperature about 1% between 10 K and RT (compared to a 10% decrease in the ionic model) is observed.

This behavior, which may look paradoxical, is in fact perfectly coherent. Due to thermal expansion, the Co $3d$ and O $2p$ hybridization, or, in other words, the number of O $2p$ holes p, is expected to decrease by increasing temperature. Since $n+p=4$, an increase of n (the total number of Co $3d$ covalent holes) will be expected, in agreement with our results.

In order to compare the obtained O $2p$ hole numbers with the changes in the Co $3d$ and O $2p$ hybridization expected from the temperature dependence of crystallographic structure,[5,8,15] we have calculated T_σ, which, in the case of the perovskite structure, is proportional[42] to $d^{3.5}/\cos(\alpha)$ (here d is the average Co-O distance[43] and α the tilting angle of the CoO_6 octahedra). Its temperature dependence, relative to the value at 10 K, is shown in Fig. 7 (solid line) together with the normalized number of O $2p$ holes $p=4-n$ (full dots). A 2% decrease of the hybridization along the σ bonds is clearly observed at higher temperatures, which agrees reasonably well with the observed diminution in the total O $2p$ hole number (about 7%) derived from our simple covalent model.

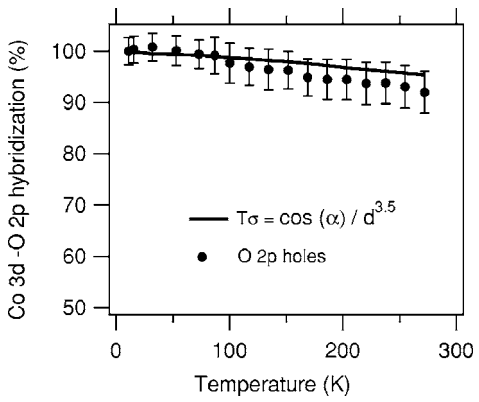

FIG. 7. Solid line: Temperature dependence of the normalized value of T_σ, $\propto\cos(\alpha)/d^{3.5}$, calculated using the structural data of Ref. 8. Full dots: Normalized O $2p$ holes, as obtained from the XAS data using the covalent model described in the text.

Because of the presence of O $2p$ holes, the e_g and t_{2g} occupations of Fig. 6(b) cannot be interpreted in terms of the ionic LS, IS, and HS configurations. According to the normalization condition $4-n(10\ \mathrm{K})=0.5$, we can, however, define a "covalent" LS state as $\mathrm{Co}t_{2g}^6e_g^{0.5}\mathrm{O}2p^{5.5}$. To be noted is that, if the polarization of the oxygen $2p$ shell compensates the moment in the e_g orbitals,[20] the spin of covalent LS will be still zero.

Looking at Fig. 6(b), it is clear that the low-temperature occupations do not correspond to this configuration, but rather to a magnetic $\mathrm{Co}t_{2g}^5e_g^{1.5}\mathrm{O}2p^{5.5}$ state that we could label as a "covalent" IS. These results contrast with those of previous studies, which agree without exception in the existence of a nonmagnetic spin state below 30 K. Although the data shown in Fig. 6 correspond to a particular choice for the Co $3d$ and O $2p$ hybridization at 10 K, the scenario does not change appreciably using slightly larger or smaller values, the main problem being the experimental observation of t_{2g} holes ($G1$ feature) already at 10 K.

The impossibility of reconciliating the existence of nonzero I_{G1} intensity and a pure LS state at low temperatures using our simple formalism is probably due to the roughness of the approximations used to describe the preedge region. It was argued earlier that the influence of the core hole is expected to be large in the K edges of $3d$ transition metals, most likely leading to a change in the hybridization of the different spin-state configurations. We, however, assumed that core hole effects did not affect covalency significatively. We also neglected the multiplet structure, as well as the contribution of the configuration with more than one hole transferred from oxygen to cobalt. We feel that these three effects should not be dismissed in further quantitative investigations.

Keeping in mind that the absolute values of the e_g and t_{2g} occupations should be considered with caution, we have calculated the spin-only effective paramagnetic moment of Co^{3+}

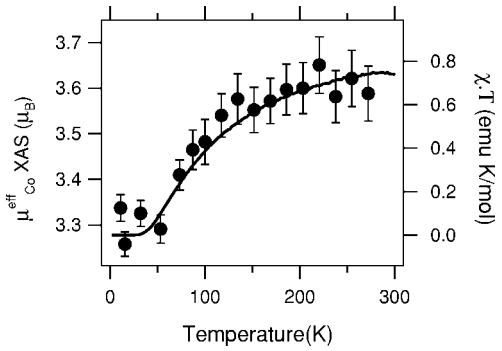

FIG. 8. Temperature dependence of the effective Co^{3+} paramagnetic moment μ^{eff} from susceptibility (solid line, right axis) and XAS (full dots, left axis).

$\mu^{eff}=2[S(S+1)]^{1/2}$ from the values of n_e and n_t displayed in Fig. 6(b) using the relationship $S=(4-n_e+n_t)/2$. The result is displayed in Fig. 8 together with the effective paramagnetic moment χ.T derived from the susceptibility. To be noted is that, in spite of the different absolute values, an excellent scaling between both sets of data is observed. The T_1 anomaly is found at the same temperature, in spite of the fact that the relevant energy levels and the final states probed by the two techniques are different (with and without core hole for XAS and χ, respectively). A comparison of the present results with O *K*-edge data obtained at low temperatures (down to 1.5 K) and increased resolution on single crystals, as well as full configuration interaction calculations on the Co *K* edge could be quite instructive in order to get a better characterization of the relevant XAS states.

V. SUMMARY AND CONCLUSIONS

We have exploited the superior resolution of PFY-XAS in new absorption measurements at the Co *K* edge of $LaCoO_3$. The increased visibility of the preedge structures, compared with that of former studies, allowed for the first time a quantitative correlation between the temperature dependence of the PFY-XAS spectra and that of the DC magnetic susceptibility. The six Co *K*-edge features identified between 7705 and 7727 eV are found to display a clear anomaly at a temperature close to $T_1=50$ K, suggesting a relationship between the observed spectroscopic changes and the magnetic transition at T_1.

In the analysis of the preedge structure, which probes the local Co 3*d* configuration, we assumed that the two observed features are mainly related to, respectively, t_{2g} and e_g states. While their anomalous intensity ratios clearly illustrate the departure from an ionic scenario, a minimal model including Co-O hybridization gives rise to much better results. The temperature dependence of both the Co 3*d* and O 2*p* hybridization and the Co magnetic moment can also be satisfactorily described within this formalism. However, due to the roughness of our approximations, the absolute values of the e_g and t_{2g} 3*d* orbitals obtained from this analysis should be considered with caution. Although this fact makes difficult a definitive statement about the nature of the involved spin states, our results are consistent with a thermally driven hole transfer from the e_g into the t_{2g} orbitals and support the existence of a transition from a lower to a higher spin state.

As is typical from high-energy spectroscopies like XAS, our inferences on the nature of the ground-state are based on the observation of transitions to highly excited states. These conclusions should be contrasted with state-of-the-art ground-state calculations and with the results of low-energy experimental probes. Also, more sophisticated models including core-hole effects, the multiplet structure, as well as the contribution of higher-energy configurations will be necessary in order to get further, quantitative insight in this fascinating and still open problem.

ACKNOWLEDGMENTS

We are grateful to J. Mesot, Ch. Bernhard, H. Luetkens, and Ch. Niedermayer for enlightening discussions as well as to the ESRF for the allocation of beam time. Financial support of the INTAS (Project No. 278) and the Swiss National Science Foundation (through the Grants SCOPES No. 7 BYPJ 065732, Marie Heim-Voegtlin No. PMPD2–102504, and the NCCR MaNEP project) is also gratefully acknowledged.

[1] C. Martin, A. Maignan, D. Pelloquin, N. Nguyen, and B. Raveau, Appl. Phys. Lett. **71**, 1421 (1997).
[2] K. Takada, H. Sakurai, E. Takayama-Muromachi, F. Izumi, R. Dilanian, and T. Sasaki, Nature (London) **422**, 53 (2003).
[3] J. B. Goodenough, J. Phys. Chem. Solids **6**, 287 (1958).
[4] C. Zobel, M. Kriener, D. Bruns, J. Baier, M. Gruninger, T. Lorenz, P. Reutler, and A. Revcolevschi, Phys. Rev. B **66**, 020402(R) (2002).
[5] G. Maris, Y. Ren, V. Volotchaev, C. Zobel, T. Lorenz, and T. T. M. Palstra, Phys. Rev. B **67**, 224423 (2003).
[6] J. Q. Yan, J. S. Zhou, and J. B. Goodenough, Phys. Rev. B **69**, 134409 (2004).
[7] W. C. Koehler and E. O. Wollan, J. Phys. Chem. Solids **2**, 100 (1957).
[8] P. G. Radaelli and S. W. Cheong, Phys. Rev. B **66**, 094408 (2002).
[9] V. G. Bhide, D. S. Rajoria, G. R. Rao, and N. R. Rao, Phys. Rev. B **6**, 1021 (1972).
[10] P. M. Raccah and J. B. Goodenough, Phys. Rev. **155**, 932 (1967).
[11] M. A. Senaris-Rodriguez and J. B. Goodenough, J. Solid State Chem. **116**, 224 (1995).
[12] K. Asai, O. Yokokura, N. Nishimori, H. Chou, J. M. Tranquada, G. Shirane, S. Higuchi, Y. Okajima, and K. Kohn, Phys. Rev. B **50**, 3025 (1994).
[13] S. Yamaguchi, Y. Okimoto, and Y. Tokura, Phys. Rev. B **55**, R8666 (1997).

[14] A. Ishikawa, J. Nohara, and S. Sugai, Phys. Rev. Lett. **93**, 136401 (2004).
[15] D. Louca, J. L. Sarrao, J. D. Thompson, H. Roder, and G. H. Kwei, Phys. Rev. B **60**, 10378 (1999).
[16] M. Abbate, J. C. Fuggle, A. Fujimori, L. H. Tjeng, C. T. Chen, R. Potze, G. A. Sawatzky, H. Eisaki, and S. Uchida, Phys. Rev. B **47**, 16124 (1993).
[17] T. Saitoh, T. Mizokawa, A. Fujimori, M. Abbate, Y. Takeda, and M. Takano, Phys. Rev. B **55**, 4257 (1997).
[18] O. Toulemonde, N. N'Guyen, F. Studer, and A. Traverse, J. Solid State Chem. **158**, 208 (2001).
[19] G. Thornton, I. W. Owen, and G. P. Diakun, J. Phys.: Condens. Matter **3**, 417 (1991).
[20] M. A. Korotin, S. Y. Ezhov, I. V. Solovyev, V. I. Anisimov, D. I. Khomskii, and G. A. Sawatzky, Phys. Rev. B **54**, 5309 (1996).
[21] R. Radwanski and Z. Ropka, Solid State Commun. **112**, 621 (1999).
[22] R. Radwanski and Z. Ropka, Physica B **281-282**, 507 (2000).
[23] Z. Ropka and R. J. Radwanski, Phys. Rev. B **67**, 172401 (2003).
[24] S. Noguchi, S. Kawamata, K. Okuda, H. Nojiri, and M. Motokawa, Phys. Rev. B **66**, 094404 (2002).
[25] A. Podlesnyak, S. Streule, J. Mesot, M. Medarde, E. Pomjakushina, K. Conder, M. Haverkort, and D. Khomskii, cond-mat/0505344 (unpublished).
[26] Z. Hu, H. Wu, M. Haverkort, H. Hsieh, H.-J. Lin, T. Lorenz, J. Baier, A. Reichl, I. Bonn, C. Felser, A. Tanaka, C. T. Chen, and L. H. Tjeng, Phys. Rev. Lett. **92**, 207402 (2004).
[27] Y. Murakami, H. Kawada, H. Kawata, M. Tanaka, T. Arima, Y. Moritomo, and Y. Tokura, Phys. Rev. Lett. **80**, 1932 (1998).
[28] Y. Murakami, J. P. Hill, D. Gibbs, M. Blume, I. Koyama, M. Tanaka, H. Kawata, T. Arima, Y. Tokura, K. Hirota, and Y. Endoh, Phys. Rev. Lett. **81**, 582 (1998).
[29] I. S. Elfimov, V. I. Anisimov, and G. A. Sawatzky, Phys. Rev. Lett. **82**, 4264 (1999).
[30] J. Q. Yan, J. S. Zhou, and J. B. Goodenough, Phys. Rev. B **70**, 014402 (2004).
[31] O. Haas, R. P. W. J. Struis, and J. M. McBreen, J. Solid State Chem. **177**, 1000 (2004).
[32] R. G. Shulman, Y. Yafet, P. Eisenberger, and W. E. Blumberg, Proc. Natl. Acad. Sci. U.S.A. **73**, 1384 (1976).
[33] J. E. Hahn, R. A. Scott, K. O. Hodgson, S. Doniach, S. R. Desjardins, and E. I. Solomon, Chem. Phys. Lett. **595**, 1982 (1982).
[34] T. E. Westre, P. Kennepohl, J. G. DeWitt, B. Hedman, K. O. Hodgson, and E. I. Solomon, J. Am. Chem. Soc. **119**, 6297 (1997).
[35] G. Draeger, R. Frahm, G. Materlik, and O. Bruemmer, Phys. Status Solidi B **146**, 287 (1988).
[36] V. Briois, C. C. dit Moulin, P. Sainctavit, C. Brouder, and A. M. Flank, J. Am. Chem. Soc. **117**, 1019 (1995).
[37] S. Ishihara and S. Maekawa, Phys. Rev. Lett. **80**, 3799 (1998).
[38] F. M. F. de Groot, M. Grioni, J. C. Fuggle, J. Ghijsen, G. A. Sawatzky, and H. Petersen, Phys. Rev. B **40**, 5715 (1989).
[39] In fact, in most 3*d* octahedral complexes the actual point symmetry of the transition metal sites is lower than O_h. In $LaCoO_3$, for example, the point symmetry at the Co positions assuming the space group $R-3c$ is -3. Though, since all six Co-O distances are equal [1.93452(6) at RT], and the O-Co-O angles differ from 90° in less than 1°, we can assume that the crystal field splitting of the 3*d* orbitals does not differ significantly from that induced by a perfect, undistorted O_h octahedral environment.
[40] L. A. Grunes, Phys. Rev. B **27**, 2111 (1983).
[41] K. Asai, P. Gehring, H. Chou, and G. Shirane, Phys. Rev. B **40**, 10982 (1989).
[42] W. Harrison, *Electronic Structure and the Properties of Solids* (Freeman, San Francisco, 1980).
[43] In spite of the differences between the crystallographic structures proposed by different authors for the high-temperature phase ($T > T_1$) (Refs. 5, 8, and 15), the average Co-O distance is nearly the same for all models. Thus, the values of $\langle d_{Co-O} \rangle$ at 100 K in the rhombohedral $R-3c$ model of Ref. 8, the Jahn-Teller distorted model of Ref. 5 and the PDF data of Louca *et al.* (Ref. 15) are respectively 1.928(1)Å, 1.926(1)Å, and 1.94(1)Å. Because only Radaelli's work provides the values of $\langle d_{Co-O} \rangle$ and α for the whole 10 K–RT temperature range, we chose this reference to calculate T_σ.